Research Note

Ostwald Ripening Stability of Curcumin-Loaded MCT Nanoemulsion: Influence of Various Emulsifiers

Sun-Hyung Kim, Yeun-Sun Ji, Eui-Seok Lee, and Soon-Taek Hong

Department of Food Science and Technology, Chungnam National University, Daejeon 34134, Korea

ABSTRACT: Curcumin is a flavonoid found in the rhizome of the turmeric plant (*Curcuma longa* L.) and has recently attracted interest because it has numerous biological functions and therapeutic properties. In the present study, we attempted to incorporate curcumin into medium-chain triglyceride (MCT) nanoemulsions (0.15 wt% curcumin, 10 wt% MCT oil, and 10 wt% emulsifiers) with various emulsifiers [polyoxyethylene (20) sorbitan monolaurate (Tween-20), sorbitan monooleate (SM), and soy lecithin (SL)]. The physicochemical properties of the nanoemulsions including the Ostwald ripening stability were investigated. The initial droplet size was found to be 89.08 nm for the nanoemulsion with 10 wt% Tween-20 (control), and when Tween-20 was partially replaced with SM and SL, the size decreased: 73.43 nm with 4 wt% SM+6 wt% Tween-20 and 67.68 nm with 4 wt% SL+6 wt% Tween-20 (prepared at 15,000 psi). When the nanoemulsions were stored for 28 days at room temperature, the droplet size increased as the storage time increased. The largest increase was observed for the control nanoemulsion, followed by the 4 wt% SL+6 wt% Tween-20 and 4 wt% SM+6 wt% Tween-20 systems. The Turbiscan dispersion stability results strongly supported the relationship between droplet size and storage time. The time-dependent increase in droplet size was attributed to the Ostwald ripening phenomenon. Thus, the Ostwald ripening stability of curcumin-loaded MCT nanoemulsions with Tween-20 was considerably improved by partially replacing the Tween-20 with SM or SL. In addition, curcumin may have acted as an Ostwald ripening inhibitor.

Keywords: curcumin, nanoemulsion, Ostwald ripening, Turbiscan, high-pressure homogenization

INTRODUCTION

Curcumin [(1E,6E)-1,7-bis(4-hydroxy-3-methoxyphenyl)-1,6-heptadiene-3,5-dione] is a flavonoid found in the rhizome of the turmeric plant (*Curcuma longa* L.), which is a member of the Zingiberaceae family. Three curcuminoid pigments contribute to the yellow color and pharmacological activities of turmeric: curcumin, demethoxycurcumin [1-(4-hydroxyphenyl)-7-(4-hydroxy-3-methoxyphenyl)-1,6-heptadiene-3,5-dione], and bisdemethoxycurcumin [1,7-bis(4-hydroxyphenyl)-1,6-heptadiene-3,5-dione] (1,2). The chemical structure of curcumin is shown in Fig. 1. Because curcumin is yellow in color, turmeric has been widely used in the food industry as a coloring agent and spice for several hundred years. Additionally, this compound has been studied because of its considerable biological and pharmaceutical activities, including anti-oxidative (3-5), anti-carcinogenic (6,7), anti-inflammatory (8-11), and anti-microbial activities (12). Because of these beneficial activities, curcumin may be a potential cure for various diseases, such as Alzheimer's disease (13, 14), Parkinson's disease (15,16), arthritis (17), and diabetes (18,19). However, curcumin is neither water-soluble nor oil-soluble (20), and when orally administered, it exhibits poor absorption (21). After oral administration
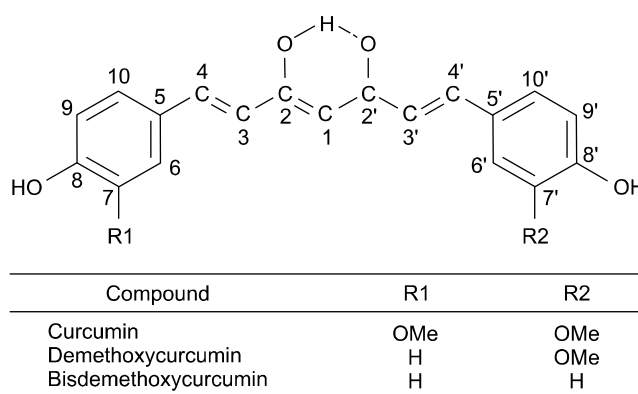

Compound	R1	R2
Curcumin	OMe	OMe
Demethoxycurcumin	H	OMe
Bisdemethoxycurcumin	H	H

Fig. 1. Chemical structure of the curcuminoid pigments. Adapted from Peret-Almeida et al. (1).

of curcumin, approximately 75% of curcumin was eliminated in the feces and low levels were found in the urine (22).

Because of the low bioavailability of functional ingredients such as curcumin, researchers have attempted to find new methods to improve water-solubility, which could enhance curcumin absorption (10). As a result, a few strategies (e.g., nanocrystals, nanosuspensions, and nanoemulsions) to improve the absorption and bioavailability of curcumin have been investigated, and the use of these systems has become popular in the functional food and nutraceutical industries over the past several years (23-25). We selected and studied nanoemulsion systems to find a stable emulsification system (e.g., conditions of emulsifiers and homogenization).

Nanoemulsions are emulsions with mean droplet sizes of 10~100 nm (26-28). Although nanoemulsions are relatively stable against physicochemical destabilization events, such as gravitational separation, flocculation, and coalescence, they become unstable over time, mainly via an Ostwald ripening phenomenon (26,29-31).

A nanoemulsion system is one of the effective strategies that can be considered to enhance the bioavailability and absorption rate in the body. Many researchers have studied oil-in-water (O/W) nanoemulsions and nanosuspensions containing bioactive or functional compounds, such as β-carotene and tocopherol. However, there have been few studies that investigated their Ostwald ripening stability with storage time. For this reason, in this study, an attempt was made to confirm whether bioactive or functional compounds such as curcumin are applicable to the emulsification system we previously established. Thus, curcumin-loaded nanoemulsions with an emulsifier system based on a previous study of Park et al. (32) were prepared. Then, we investigated the Ostwald ripening stability of the curcumin-loaded nanoemulsions during storage.

MATERIALS AND METHODS

Materials
Curcumin and polyoxyethylene (20) sorbitan monolaurate (Tween-20) were purchased from Sigma-Aldrich Co. (St. Louis, MO, USA). Medium-chain triglyceride (MCT) oil, sorbitan monooleate (SM), and soy lecithin (SL) were provided by ILSHIN WELLS Co., Ltd. (Seoul, Korea). In the present study, Tween-20, SM, and SL were used as emulsifiers. Other chemicals used were of analytical grade.

Preparation of curcumin-loaded nanoemulsions
Emulsions were prepared using the modified method of Ahmed et al. (33). The emulsifier systems used were based on the results of Park et al. (32) and were as follows: 10 wt% Tween-20 (control), 4 wt% SM+6 wt% Tween-20, and 4 wt% SL+6 wt% Tween-20. The total amount of each emulsifier (Tween-20, SM, and SL) was fixed at 10 wt%, and each was dissolved into the appropriate phase (aqueous or oil) depending on its polarity. An aqueous phase was prepared with 20 mM bis-tris buffer (0.02 wt% sodium azide, pH 7.0) and the hydrophilic emulsifier (Tween-20). Curcumin (0.15 wt% in emulsion) was added to the MCT oil and dissolved at 70 °C with constant stirring and sonication. The lipophilic emulsifiers (SM and SL) were added to a curcumin-containing oil phase, which was then stirred at 70°C for 30 min. The aqueous and oil phases were premixed using a L4RT mixer (L4RT, Silverson Machines Ltd., Chesham, UK) at 8,000 rpm for 5 min. This premix was homogenized by M-110Y (Microfluidics, Newton, MA, USA) at various pressures (5,000, 10,000, and 15,000 psi) for 4 cycles to prepare the final O/W nanoemulsions (10 wt% emulsifier, 10 wt% oil, and 20 mM bis-tris buffer).

Measurements of droplet size in curcumin-loaded nanoemulsions
The droplet size in the curcumin-loaded nanoemulsions was measured by dynamic light scattering using a laser particle size analyzer (Zetasizer Nano ZS, Malvern Instruments Ltd., Malvern, UK). Emulsion samples were diluted 1,000-fold with 20 mM bis-tris buffer (0.02 wt% sodium azide, pH 7.0) to avoid multiple light scattering. The measurements were performed in triplicate at room temperature.

Emulsion stability measurements of curcumin-loaded nanoemulsions by Turbiscan
The Turbiscan (Turbiscan[TM] Lab., Formulaction, L'Union, France) is an instrument that can evaluate dispersion or emulsion stability through multiple light-scattering phenomena without sample dilution. In this system, the emulsion stability was analyzed by the following procedure: Near-infrared light of approximately 880 nm is scanned through a glass vial containing the emulsion sample by moving upward and downward. During this scan, variations in the transmittance and backscattering intensities induced by the light applied to the dispersed phase during the test are measured simultaneously. If destabilization occurs, such as particle migration (creaming or sedimentation) or particle size variation (flocculation or coalescence), the flux of the radiation that is transmitted through or backscattered by the droplets changes accordingly. Therefore, the dispersion or emulsion stability can be estimated (34). The measurement time can be arbitrarily determined depending on the stability and physical properties of the emulsion or dispersion. In the present study, the emulsion stability was monitored for 3

days to give enough time for the stability measurements.

Statistical analysis

The measurements in this study were performed in duplicate or triplicate. Experimental data were treated by analysis of variance (ANOVA) using SAS 9.4 for Windows (SAS Inc., Cary, NC, USA) and the results were expressed as the mean values and the standard deviation. Significant differences between the means were determined by Duncan's multiple range test.

RESULTS AND DISCUSSION

Initial droplet size in curcumin-loaded nanoemulsions

Curcumin-loaded nanoemulsions with various emulsifiers prepared with various emulsifiers under high-pressure homogenization conditions of 15,000 psi and 4 cycles are shown in Fig. 2 and the initial (after 1 day) droplet sizes of curcumin-loaded nanoemulsions with various emulsifiers are shown in Table 1. In all of the curcumin-loaded nanoemulsions, the initial droplet size tended to decrease as the homogenizing pressure increased from 5,000 to 15,000 psi. In addition, a smaller initial droplet size was observed when Tween-20 was partially replaced with SM or SL: 89.08 nm with 10 wt% Tween-20, 73.43 nm with 4 wt% SM+6 wt% Tween-20, and 67.68 nm with 4 wt% SL+6 wt% Tween-20 when prepared at 15,000 psi. According to Kolmogorov's theory (35), the key factor that controls efficient homogenization is the high power input (i.e., the homogenizing pressure). Furthermore, the homogenizing pressure has been shown to affect the droplet radius; thus, a relationship exists between the homogenizing pressure and the droplet radius (36-38). This relationship explains why applying higher homogenizing pressures produces nanoemulsions with smaller droplet

Fig. 2. Curcumin-loaded nanoemulsions prepared with various emulsifiers under high-pressure homogenization conditions of 15,000 psi and 4 cycles. (left: Tween-20 only, middle: Tween-20+SM, and right: Tween-20+SL). Tween-20, polyoxyethylene (20) sorbitan monolaurate; SM, sorbitan monooleate; SL, soy lecithin.

sizes. It is generally accepted that emulsion stability is enhanced when a hydrophilic emulsifier is used in combination with a hydrophobic one (38), possibly because doing so reinforces the interfacial layer. This reinforced interfacial layer contributes to the prevention of coalescence between droplets in the emulsions (39). In the present study, therefore, smaller droplet sizes in the emulsions with Tween-20+SM or SL can be expected.

Changes of droplet size in curcumin-loaded nanoemulsions during storage time

Changes in droplet size in curcumin-loaded nanoemulsions prepared under various conditions (i.e., different homogenizing pressures and emulsifier systems) versus storage time are shown in Fig. 3 and Table 1. When the nanoemulsions were stored at room temperature for 28

Table 1. Droplet size and polydispersity of curcumin-loaded nanoemulsions prepared with various emulsifier systems at different homogenizing pressures

Homogenizing pressure (psi)	Ratio of surfactants[1] (wt %)	Droplet size (nm) after 1 day	PdI[2]	Droplet size (nm) after 28 days	PdI
5,000	Tween-20 (10)	106.97±0.90[a]	0.139±0.012[a]	121.80±1.36[a]	0.096±0.013[b]
	Tween-20 : SM (6:4)	89.13±0.34[c]	0.097±0.004[b]	94.71±0.44[c]	0.110±0.005[ab]
	Tween-20 : SL (6:4)	105.50±0.33[b]	0.135±0.004[a]	109.30±0.51[b]	0.124±0.009[a]
10,000	Tween-20 (10)	85.85±0.60[a]	0.160±0.005[a]	111.37±0.45[a]	0.104±0.004[a]
	Tween-20 : SM (6:4)	77.44±0.39[b]	0.098±0.002[c]	82.24±0.29[c]	0.106±0.017[a]
	Tween-20 : SL (6:4)	77.21±0.35[b]	0.146±0.007[b]	86.33±0.39[b]	0.131±0.008[a]
15,000	Tween-20 (10)	89.08±0.85[a]	0.137±0.013[a]	109.23±0.42[a]	0.114±0.010[b]
	Tween-20 : SM (6:4)	73.43±0.48[b]	0.081±0.017[b]	77.38±0.11[b]	0.084±0.011[c]
	Tween-20 : SL (6:4)	67.68±0.32[c]	0.143±0.014[a]	77.88±0.14[b]	0.141±0.005[a]

Values represent mean±SD (n=3).
Means with the different letters (a-c) within same column of each homogenizing pressure are significantly different (*P*<0.01) according to Duncan's multiple range test.
[1]Tween-20, polyoxyethylene (20) sorbitan monolaurate; SM, sorbitan monooleate; SL, soy lecithin.
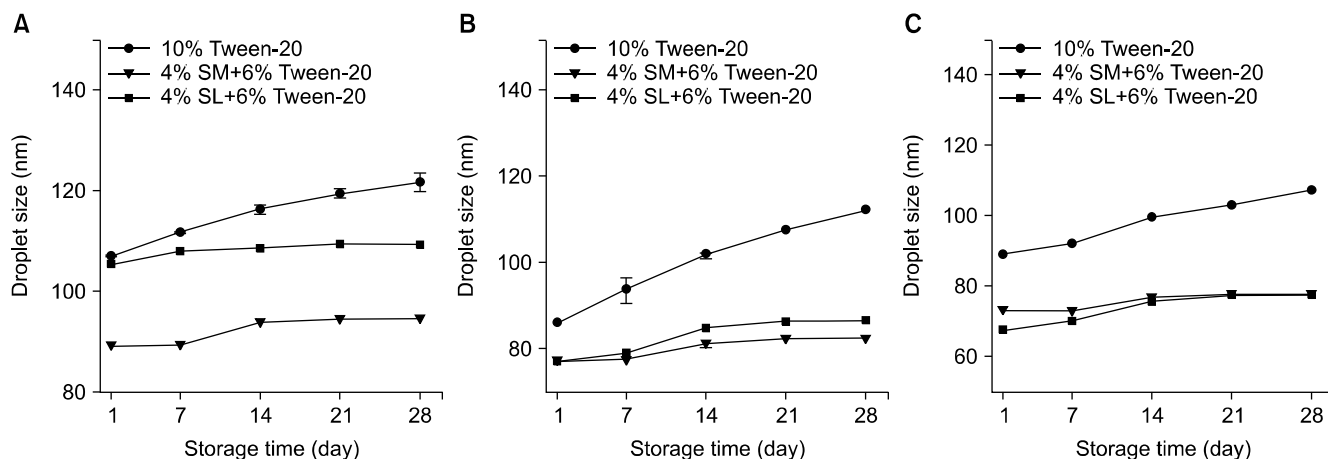[2]PdI, polydispersity index.

Fig. 3. Changes in droplet size in curcumin-loaded nanoemulsions (10 wt% emulsifier, 10 wt% oil, and 20-mM bis-tris buffer) with storage time. The emulsions were prepared at various pressure [(A) 5,000 psi, (B) 10,000 psi, and (C) 15,000 psi]. Tween-20, polyoxyethylene (20) sorbitan monolaurate; SM, sorbitan monooleate; SL, soy lecithin.

days, droplet size gradually increased with storage time, possibly because of Ostwald ripening (32). The largest increase at 15,000 psi was observed for the control nanoemulsion, followed by the 4 wt% SL+6 wt% Tween-20 system and the 4 wt% SM+6 wt% Tween-20 system (Table 1). A similar tendency was observed by Park et al. (32).

Ostwald ripening rate

Ostwald ripening in O/W emulsions is primarily attributable to the solubility of the dispersed phase (oil phase) in the continuous phase (aqueous phase) (40). The Ostwald ripening rate can be derived from the Lifshitz-Slyozov-Wagner (LSW) theory (41).

$$d(t)^3 - d(0)^3 = \omega t = \frac{32}{9} \alpha S_\infty D t$$

where d(t) is the mean droplet size at time (t), d(0) is the initial droplet size, ω is the Ostwald ripening rate, D is the translation diffusion coefficient of the dispersed phase, S_∞ is the bulk solubility of the dispersed phase in the continuous phase, and α is the characteristic length scale ($\alpha = 2\gamma V_m/RT$). According to this equation, the cube of droplet size [d(t)^3] exhibits a linear relation with t, and thus ω of the nanoemulsions is the slope of the straight line of the linear regression. ω of the curcumin-loaded nanoemulsions calculated using the above equation are presented in Table 2. This table shows that the control nanoemulsion had the fastest Ostwald ripening rate (i.e., highest ω), and partially replacing Tween-20 with SM or SL resulted in the nanoemulsion with lower ω compared to the control. This finding is attributable to the emulsifying properties of SM, which is a lipophilic emulsifier with a hydrophile-lipophile balance (HLB) value of 4.30. Apparently, SM retarded the diffusion of the relatively highly water-soluble MCT oil toward the con-

Table 2. Ostwald ripening rates (ω) of curcumin-loaded nanoemulsions prepared with various emulsifier systems at different homogenizing pressures

Homogenizing pressure (psi)	Ratio of surfactants[1] (wt %)	ω [×10^4] (nm)^3/h	R^2
5,000	Tween-20 (10)	9.07	0.9808
	Tween-20 : SM (6:4)	2.54	0.8446
	Tween-20 : SL (6:4)	1.91	0.8292
10,000	Tween-20 (10)	11.65	0.9953
	Tween-20 : SM (6:4)	1.72	0.8457
	Tween-20 : SL (6:4)	3.16	0.8972
15,000	Tween-20 (10)	9.68	0.9876
	Tween-20 : SM (6:4)	1.32	0.7879
	Tween-20 : SL (6:4)	2.76	0.9022

[1]Tween-20, polyoxyethylene (20) sorbitan monolaurate; SM, sorbitan monooleate; SL, soy lecithin.

tinuous phase by forming an interfacial layer, possibly from inside the droplets, during the emulsification process (42). In addition, the nanoemulsion with only Tween-20 produced at 5,000 psi generally exhibited a lower ω than those prepared at 10,000 and 15,000 psi. This difference can be attributed to the droplet size in the nanoemulsions because Ostwald ripening proceeds more rapidly when the initial droplet size is smaller (43).

In general, the Ostwald ripening rates we observed were lower than those reported by Park et al. (32) for systems of nanoemulsions that were not loaded with curcumin. This difference can be explained by a phenomenon that is discussed below. When an O/W emulsion contains droplets composed of two components with different water-solubilities (i.e., water-insoluble and appreciable water-soluble), one component with an appreciable high water-solubility will diffuse from small droplets to large droplets due to Ostwald ripening (39). Consequently, this leads to differences in droplet composition—higher concentration of water-insoluble component in the

smaller droplets than in the large ones. However, this difference is thermodynamically unfavorable because of the entropy of mixing generated by a component with water-insoluble one. Therefore, the Ostwald ripening rates would be reduced.

In other words, by mixing a substance with low water-solubility (e.g., curcumin) with an oil that has an appreciable water-solubility (e.g., MCT) at a certain ratio, the Ostwald ripening rate can be reduced by the thermodynamic driving force (entropy of mixing effect); this phenomenon is usually referred to as compositional ripening (40). Lim et al. (44) reported that the increase in mean droplet size of O/W emulsions containing orange oil (high water-solubility component) due to Ostwald ripening was retarded during storage time by adding ester gum (low water-solubility component). This is because the ester gum acts as a ripening inhibitor, effectively retarding Ostwald ripening, and the droplet growth was completely inhibited when ester gum concentration in the oil phase exceeds 10%. Walstra (43) also reported
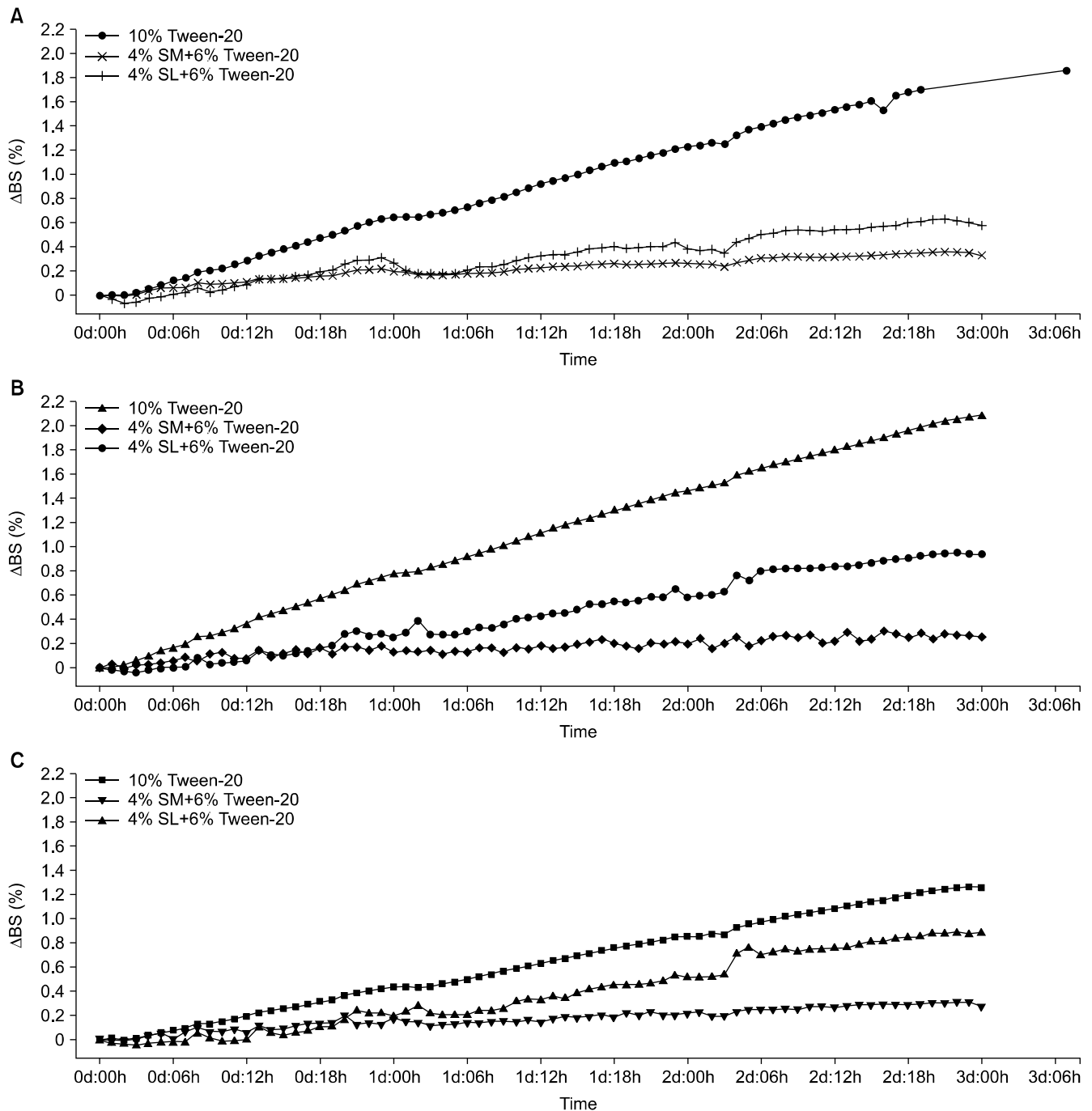

Fig. 4. Changes in the backscattering profiles of the curcumin-loaded nanoemulsions measured using a Turbiscan system for 3 days. (A) 5,000 psi, (B) 10,000 psi, and (C) 15,000 psi. $\Delta BS = BS_t - BS_0$. BS_t, backscattering intensity at time=t; BS_0, backscattering intensity at time=0. Tween-20, polyoxyethylene (20) sorbitan monolaurate; SM, sorbitan monooleate; SL, soy lecithin.

that Ostwald ripening stability could be similarly improved in water-in-oil (W/O) emulsions by introducing water-soluble components (i.e., salts) with low lipid-solubility into the continuous phase (42). In the present study, curcumin might have also acted as an Ostwald ripening inhibitor (low water-solubility component), thereby retarding Ostwald ripening.

Stability evaluation of curcumin-loaded nanoemulsions by Turbiscan

The stability of curcumin-loaded nanoemulsions was evaluated using a Turbiscan system for 3 days, as shown in Fig. 4. The changes in the backscattering intensity (ΔBS) were expressed as a function of time. The ΔBS (%) values of the nanoemulsions with Tween-20 only, Tween-20 partially replaced with SL, and Tween-20 partially replaced with SM were approximately 1.75, 0.60, and 0.30 at 5,000 psi; 2.10, 0.90, and 0.30 at 10,000 psi; and 1.30, 0.89 and 0.30 at 15,000 psi, respectively. These values generally coincided with the increasing tendencies of droplet size and Ostwald ripening rate. Therefore, these differences in ΔBS likely resulted from Ostwald ripening, which may be especially problematic in nanoemulsions containing short-chain triglyceride or MCT oils (38).

CONCLUSION

This study was performed to evaluate the Ostwald ripening stability of curcumin-loaded nanoemulsions prepared using various emulsifier systems established by Park et al. (32). Ostwald ripening has been shown to be influenced by several factors, such as droplet size and its distribution, solubility of the dispersed phase, interfacial tension, interfacial diffusion, and droplet composition (40). Additionally, the emulsion stability of O/W emulsions has been empirically shown to be maximized by the use of surfactants with HLB values in the range of 10~12 (45). Similarly, in this study, an emulsifier system (4 wt% SM +6 wt% Tween-20) with an emulsifier with a HLB value of 11.74 exhibited the best stability against Ostwald ripening, followed by those of the 4 wt% SL+6 wt% Tween-20 system and the 10 wt% Tween-20 system (HLB value of 16.70). The results from this study clearly demonstrate that using the emulsifier systems of Park et al. (32) could produce nanoemulsions exhibiting similar trends in Ostwald ripening stability. Moreover, ω of curcumin-loaded nanoemulsion was lower than that of nanoemulsions without curcumin. Thus, curcumin may have retarded Ostwald ripening by acting as an Ostwald ripening inhibitor (i.e., a low water-solubility substance). The results from the present study will significantly contribute to controlling the Ostwald ripening phenomenon in nanoemulsions containing bioactive and functional compounds.

AUTHOR DISCLOSURE STATEMENT

The authors declare no conflict of interest.

REFERENCES

1. Péret-Almeida L, Cherubino APF, Alves RJ, Dufossé L, Glória MBA. 2005. Separation and determination of the physico-chemical characteristics of curcumin, demethoxycurcumin and bisdemethoxycurcumin. *Food Res Int* 38: 1039-1044.
2. Bong PH. 2000. Spectral and photophysical behaviors of curcumin and curcuminoids. *Bull Korean Chem Soc* 21: 81-86.
3. Sharma OP. 1976. Antioxidant activity of curcumin and related compounds. *Biochem Pharmacol* 25: 1811-1812.
4. Ak T, Gülçin I. 2008. Antioxidant and radical scavenging properties of curcumin. *Chem Biol Interact* 174: 27-37.
5. Ruby AJ, Kuttan G, Babu KD, Rajasekharan KN, Kuttan R. 1995. Anti-tumour and antioxidant activity of natural curcuminoids. *Cancer Lett* 94: 79-83.
6. Kuttan R, Bhanumathy P, Nirmala K, George MC. 1985. Potential anticancer activity of turmeric (*Curcuma longa*). *Cancer Lett* 29: 197-202.
7. Huang MT, Lou YR, Ma W, Newmark HL, Reuhl KR, Conney AH. 1994. Inhibitory effects of dietary curcumin on forestomach, duodenal, and colon carcinogenesis in mice. *Cancer Res* 54: 5841-5847.
8. Huang HC, Jan TR, Yeh SF. 1992. Inhibitory effect of curcumin, an anti-inflammatory agent, on vascular smooth muscle cell proliferation. *Eur J Pharmacol* 221: 381-384.
9. Srimal RC, Dhawan BN. 1973. Pharmacology of diferuloyl methane (curcumin), a non-steroidal anti-inflammatory agent. *J Pharm Pharmacol* 25: 447-452.
10. Wang X, Jiang Y, Wang YW, Huang MT, Ho CT, Huang Q. 2008. Enhancing anti-inflammation activity of curcumin through O/W nanoemulsion. *Food Chem* 108: 419-424.
11. Duvoix A, Blasius R, Delhalle S, Schnekenburger M, Morceau F, Henry E, Dicato M, Diederich M. 2005. Chemopreventive and therapeutic effects of curcumin. *Cancer Lett* 223: 181-190.
12. Negi PS, Jayaprakasha GK, Jagan Mohan Rao L, Sakariah KK. 1999. Antibacterial activity of turmeric oil: a byproduct from curcumin manufacture. *J Agric Food Chem* 47: 4297-4300.
13. Ringman JM, Frautschy SA, Cole GM, Masterman DL, Cummings JL. 2005. A potential role of the curry spice curcumin in Alzheimers disease. *Curr Alzheimer Res* 2: 131-136.
14. Lim GP, Chu T, Yang F, Beech W, Frautschy SA, Cole GM. 2001. The curry spice curcumin reduces oxidative damage and amyloid pathology in an Alzheimer transgenic mouse. *J Neurosci* 21: 8370-8377.
15. Mythri RB, Bharath MMS. 2012. Curcumin: a potential neuroprotective agent in Parkinson's disease. *Curr Pharm Des* 18: 91-99.
16. Jagatha B, Mythri RB, Vali S, Bharath MMS. 2008. Curcumin treatment alleviates the effects of glutathione depletion *in vitro* and *in vivo*: therapeutic implications for Parkinson's disease explained via in silico studies. *Free Radic Biol Med* 44: 907-917.
17. Jackson JK, Higo T, Hunter WL, Burt HM. 2006. The antioxi-

dants curcumin and quercetin inhibit inflammatory processes associated with arthritis. *Inflamm Res* 55: 168-175.

18. Zhang DW, Fu M, Gao SH, Liu JL. 2013. Curcumin and diabetes: a systematic review. *Evid Based Complement Alternat Med* 2013: 636053.

19. Chiu J, Khan ZA, Farhangkhoee H, Chakrabarti S. 2009. Curcumin prevents diabetes-associated abnormalities in the kidneys by inhibiting p300 and nuclear factor-κB. *Nutrition* 25: 964-972.

20. Tønnesen HH, Másson M, Loftsson T. 2002. Studies of curcumin and curcuminoids. XXVII. Cyclodextrin complexation: solubility, chemical and photochemical stability. *Int J Pharm* 244: 127-135.

21. Maiti K, Mukherjee K, Gantait A, Saha BP, Mukherjee PK. 2007. Curcumin-phospholipid complex: preparation, therapeutic evaluation and pharmacokinetic study in rats. *Int J Pharm* 330: 155-163.

22. Wahlström B, Blennow G. 1978. A study on the fate of curcumin in the rat. *Acta Pharmacol Toxicol* 43: 86-92.

23. Chen H, Weiss J, Shahidi F. 2006. Nanotechnology in nutraceuticals and functional foods. *Food Technol* 60: 30-36.

24. Weiss J, Takhistov P, McClements DJ. 2006. Functional materials in food nanotechnology. *J Food Sci* 71: R107-R116.

25. Kreilgaard M. 2002. Influence of microemulsions on cutaneous drug delivery. *Adv Drug Delivery Rev* 54: S77-S98.

26. McClements DJ, Rao J. 2011. Food-grade nanoemulsions: formulation, fabrication, properties, performance, biological fate, and potential toxicity. *Crit Rev Food Sci Nutr* 51: 285-330.

27. McClements DJ. 2012. Nanoemulsions versus microemulsions: terminology, differences, and similarities. *Soft Matter* 8: 1719-1729.

28. Mason TG, Wilking JN, Meleson K, Chang CB, Graves SM. 2006. Nanoemulsions: formation, structure, and physical properties. *J Phys Condens Matter* 18: R635-R666.

29. Tadros T, Izquierdo P, Esquena J, Solans C. 2004. Formation and stability of nano-emulsions. *Adv Colloid Interface Sci* 108-109: 303-318.

30. Wooster TJ, Golding M, Sanguansri P. 2008. Impact of oil type on nanoemulsion formation and Ostwald ripening stability. *Langmuir* 24: 12758-12765.

31. Dickinson E. 1992. *Introduction to food colloids*. Oxford University Press, Oxford, UK. p 109-110.

32. Park EJ, Lee ES, Hong ST. 2015. A study on the formation and Ostwald ripening stability of nanoemulsion with various emulsifiers. *J of Korean Oil Chemists' Soc* 32: 536-545.

33. Ahmed K, Li Y, McClements DJ, Xiao H. 2012. Nanoemulsion- and emulsion-based delivery systems for curcumin: encapsulation and release properties. *Food Chem* 132: 799-807.

34. Mengual O, Meunier G, Cayré I, Puech K, Snabre P. 1999. TURBISCAN MA 2000: multiple light scattering measurement for concentrated emulsion and suspension instability analysis. *Talanta* 50: 445-456.

35. Dickinson E. 1992. *Introduction to food colloids*. Oxford University Press, Oxford, UK. p 115-119.

36. Walstra P, Smulders PEA. 1988. Emulsion formation. In *Modern Aspects of Emulsion Science*. Binks BP, ed. Royal Society of Chemistry, Information Services, Cambridge, UK. p 56-99.

37. Stang M, Schuchmann H, Schubert H. 2001. Emulsification in high-pressure homogenizers. *Eng Life Sci* 1: 151-157.

38. Yoon SH, Choe EO, Song YO, Oh CH, Jung MY, Hong ST, Chang PS, Lee JH, Kim HJ. 2015. *Food lipids*. Hong ST, ed. Soohaksa, Seoul, Korea. p 247-297.

39. McClements DJ. 2015. *Food emulsions: principles, practice, and techniques*. 3rd ed. CRC Press, Boca Raton, FL, USA. p 342-346.

40. McClements DJ. 2015. *Food emulsions: principles, practice, and techniques*. 3rd ed. CRC Press, Boca Raton, FL, USA. p 358-365.

41. Kabalnov AS, Shchukin ED. 1992. Ostwald ripening theory: applications to fluorocarbon emulsion stability. *Adv Colloid Interface Sci* 38: 69-97.

42. Xin X, Zhang H, Xu G, Tan Y, Zhang J, Lv X. 2013. Influence of CTAB and SDS on the properties of oil-in-water nanoemulsion with paraffin and span 20/Tween 20. *Colloids Surf A* 418: 60-67.

43. Walstra P. 2003. *Physical chemistry of foods*. Marcel Dekker, Inc., New York, NY, USA. p 450-462.

44. Lim SS, Baik MY, Decker EA, Henson L, Popplewell LM, McClements DJ, Choi SJ. 2011. Stabilization of orange oil-in-water emulsions: A new role for ester gum as an Ostwald ripening inhibitor. *Food Chem* 128: 1023-1028.

45. McClements DJ. 2005. *Food emulsions: principles, practice, and techniques*. 2nd ed. CRC Press, Boca Raton, FL, USA. p 131-133.